A convective model for laboratory fires with well-ordered vertically-oriented fuel beds

François Joseph Chatelon, Jacques Henri Balbi, Dominique Morvan, Jean Louis Rossi, Thierry Marcelli

A convective model for laboratory fires with well-ordered vertically-oriented fuel beds

François Joseph Chatelon[a], Jacques Henri Balbi[a], Dominique Morvan[b], Jean Louis Rossi[a], Thierry Marcelli[a,*]

[a] *Université de Corse, Systèmes Physiques pour l'Environnement UMR-CNRS 6134, Campus Grossetti, BP 52 20250 Corte, France*
[b] *Aix Marseille Univ, CNRS, Centrale Marseille, M2P2, Marseille, France*

Several studies in the literature explore the connection between rate of spread (ROS) and wind in wildland fires. These studies show very different positions about the role of radiation and convection as heat transfer mechanisms. In the case when the fuel bed is well-ordered and vertically-oriented, there seems to be a consensus leading to suggest that convective heating is the dominant heat transfer mode in that case. The purpose of this work is to propose a convective semi-physical model for the behaviour of the rate of spread in wind, when the fuel bed is vertically-oriented. Due to a specific fuel bed arrangement, flame radiation –i.e. radiation from the part of the flame above the vegetal stratum– is neglected. Only horizontal radiation from the fuel burning particles area and convective heating are taken into account. Convective heat transfer is assumed to be the primary heat transfer mechanism. The proposed model is confronted to 172 laboratory fires with a wide range of fuel characteristics. The predicted results are also compared with two simplified models from the literature. Statistical tools are used to check the agreement between the predicted ROS and the observed one where a strong agreement is generally observed, irrespective of fuel bed characteristics.

1. Introduction

Wind is commonly accepted [1] as one of the major factors that affects a fire is rate of spread. Generally, fire burning aided by wind expresses higher rates of spread than in 'no-wind' cases. Several studies have described the relationship between the ROS R and wind velocity U, where a power function of the wind velocity ($R \propto U^n$) is commonly fitted to ROS data [2,3]. The exponent n derived from these studies, however, is inconsistent. For instance, Thomas and Pickard [4], Wolff et al. [5] and Catchpole et al. [6], observed $n < 1$ whereas the results provided by Rothermel and Anderson [7], Rothermel [8], or Mendes-Lopes et al. [9] suggested $n > 1$. All these cases are part of what Rothermel and Anderson [7] presented as the three possible curve shapes for ROS in wind conditions.

The main heat transfer mechanism induced by fuel bed geometries seems to be important in order to explain those different curve shapes. Indeed, fire spread models commonly assume a steady spread [8,10,11], and the interface between burning and preheating fuel related to fire spread has been widely studied, especially for shallow and continuous fuel beds [8,12,13]. Radiant heat transfer from the flame to the unburnt fuel has been widely considered as the primary mechanism controlling fire spread, the heating and ignition of fuel particles by flame contact being largely neglected [14]. However, Anderson [15], Fang [16] for surface fires, and Van Wagner [17] for crown fires, indicated that the radiant heat transfer could only account for a part of the total heat flux necessary to sustain a spreading fire. Some authors [18,19] also found that radiation heat transfer was not sufficient to ignite fuel bed particles due to the too low fuel particles temperature at the flame's arrival. Note also that some recent results on the wildland fire flame spread and ignition mechanisms detail the location where the local heat flux received by downstream surface in wind-driven fires is maximum [20].

At the field scale, some fuels display discontinuities between individual plants. In order to investigate the fire behaviour in these fuel types, some authors have proceeded to laboratory experiments where fuel beds are made of well-ordered, vertically oriented particles with regular spacing. These fuel beds are usually constituted by matchsticks [12,21,22], toothpicks [5] or laser-cut cardboard [23]. For those discontinuous fuel beds, *i.e.* fuel beds with significant gaps between individual fuel elements, it has been suggested that convective heat transfer is necessary to correctly understand the fire spread mechanisms [2,3,19,24,25]. Finney et al. [14] also conclude that the

* Corresponding author.
E-mail address: marcelli@univ-corse.fr (T. Marcelli).

ignition of fuel particles after direct contact is the main mechanism thanks to which the fire propagates.

In a recent work [26], Finney et al. focused on the role of convective and radiative heating on fire spread. Their measurements performed on a set of experiments conducted on those discontinuous fuel beds show that radiation causes a slow increase of the fuel temperature whose value remains below 100 °C. Moreover, when bursts of flame and hot gases contact intermittently the unburnt fuel particles, fuel temperature increases fastly. In this type of fuel bed arrangement, convective heating seems to be the main heat transfer mechanism.

The main purpose of this paper is to present a simplified semi-physical model which is able to correctly reproduce the ROS in wind conditions, when the fuel bed is well-ordered and vertically-oriented. The main phenomena in fire spreading are represented by some physical laws, but nevertheless some empirical laws could be added. By using some approximations, this model tries to solve, the equations governing heat transfer and combustion, and as such can be classified as a simplified semi-physical model. Particularly, these simplifying assumptions avoid into account taking the gas transport equations explicitly, which leads to a model constituted by algebraic equations with two advantages: a computational time close to zero and an explicit analytic relationship giving the ROS as a function of the wind velocity and the main characteristics of the vegetal stratum and the environment. Among the three usual heat transfer modes, flame radiation –the radiation from the part of the flame located above the vegetal stratum– is neglected because it is weakly received by the fuel particles due to their verticality –following the work of Finney et al. [26]. Radiation from the flame base –fuel burning particles area– is obtained thanks to the assumption of an equivalent radiant panel. Because of the weak packing ratio and the well-ordered geometry of the fuel bed, the air flow easily enters the vegetal stratum and a part of this flow is going to go out through the flame base-unburnt fuel bed interface. Then the convective effects with direct flame contact are assumed to be important and represent the main heat transfer mechanism. This assumption is supported by the work of Finney et al. [26]. Obviously, in the case of a continuous fuel bed, radiation cannot be neglected and may often control the flame spread, especially with large fires.

In a first section, the main equations of the model are set. Especially, horizontal and vertical velocities of the gaz flow in the vegetal stratum are estimated, which involves the divided streamline: gases get out of the flame base through its upper part or by the flame base-unburnt fuel interface. An assessment of the contact flame power and its absorbed part for the fuel preheating is done. Finally, according to Balbi et al. [27], a thermal balance on the preheating fuel bed gives the expression of the ROS.

This convective model is composed of three universal model parameters –set up on two experiments– and their value is the same whatever the experiment series.

In a second section, the model is confronted to several sets of laboratory experiments and is compared to two other empirical models found in the literature, namely the simplified models provided by Wolff et al. [5] and Catchpole et al. [6]. The effectiveness of the model is evaluated with usual statistical tools, such as the normalized mean square error (NMSE), the fractional bias (FB), and the Pearson correlation coefficient (r).

2. Main equations of the model

In order to obtain a simplified model, it is necessary to process complex phenomena in a simple way. Particularly, the gases movement in and around the flame is considered to be stochastic, but its effects on the rate of spread are completely deterministic. The proposed model is obtained by considering mean movements in time and space, so equivalent laminar flows are used in the place of turbulent flows and the main physical characteristics of the fire front (temperature, flame height...) are replaced with mean values. The fire front is considered to be a linear one.

2.1. Stream lines

Pyrolysis gases are emitted from the flame base, i.e. the fuel burning particles area –denoted by ABCD in Fig. 1. The temperature in the preheating zone (BB'C'C in Fig. 1), which is close to the one suggested by Pitts [2], ranges from ambient temperature to ignition temperature. The air stream which comes from the burnt area crosses the flame base and mixes with pyrolysis gases is subjected to progressive drag forces and driven to the top of the flame base, due to buoyancy. Due to the low fuel bed density and the vertical arrangement of the fuel particles, the drag forces are weak compared to a continuous fuel bed. So the stream lines will go out through the front panel of the flame base –denoted by BC in Fig. 1– or through the top of the flame base –denoted by AB in Fig. 1. Those two air streams are split by the line denoted by EB in Fig. 1. So, the flame can be divided in two parts, an external part above the vegetal stratum and an internal part which directly contacts the unburnt fuel bed and which will give the major part of energy transfer. The existence of this internal part of the flame has been emphasized by temperature measurements [28] or gas velocity measurements [29] in the fuel bed.

Therefore, the flame contour is determined by the intersection of the flame base with stream lines number 1 and 3 (Fig. 1). The plume is

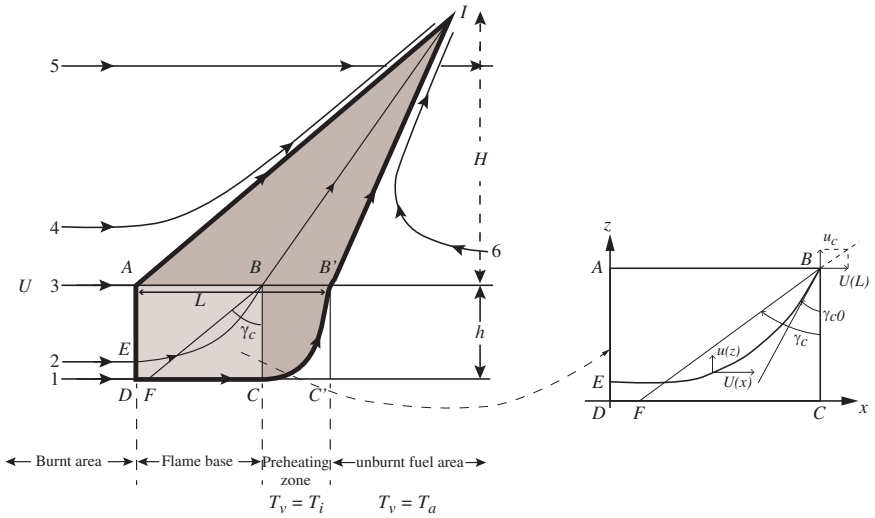

Fig. 1. Flaming zone combustion profile in presence of wind in the normal direction.

considered to be above the top of the flame (point I in Fig. 1). The stream lines above the flame body (number 4 in Fig. 1) follow the flame shape. In the same way, a fresh airflow (number 6 in Fig. 1) coming from the unburnt area, under the flame body also follows the flame shape. Indeed, in this area, the quasi-laminar flame acts as a barrier to the fresh wind stream. However, the flame is unsteady and discontinuous and external air movement can go through these discontinuities (number 5 in Fig. 1). The energy contribution of those stream lines is neglected because of their distance from the fuel bed and because of their temperature which is close to the ambient temperature.

On the other hand, all the stream lines located between number 1 and number 2 (Fig. 1) create an internal part of the flame –with the pyrolysis gases– (BCB' in Fig. 1) which will contribute to the unburnt fuel bed preheating. Then, it is necessary to quantify this heating energy which means to estimate the surface bounded by stream lines number 1 and 2. It is also necessary to quantify the part of the energy caught by the fuel bed. On the one hand, the external part of the flame (AIB') does not contribute to the preheating and on the other hand, there is no convective cooling coming from the unburnt area, but there might be a lateral convective cooling –coming from the face BB'C'C– in case of absent lateral walls.

2.2. Gas velocity modelling

In order to determine horizontal gas velocity, an empirical law is used to model drag forces. Indeed, as the air stream progresses through the fuel bed, drag forces –which are assumed to be proportional to the square of the normal wind velocity U^2– become more and more important, thus resulting in the differential equation $U(x)\,dU(x)/dx = -K^*U^2(x)$, where K^* is a coefficient and $U(x)$ the stream velocity within the fuel bed at the fuel bed length x (Table 1).

Solving this differential equation leads to the following solution:

$$U(x) = U(0)e^{-Kx} \tag{1}$$

Anderson et al. [29] observed this decrease in $U(x)$ at the top of the vegetal stratum in a region close to the flame front.

Upward gas velocity is due to buoyancy forces which result in a uniformly accelerated motion. An estimation –at mid-height vegetal stratum– is obtained with the simplified balance of the momentum equation in the vertical direction and is given by

$$u^2(z) = 2g\left(\frac{T_m}{T_a}-1\right)z \tag{2}$$

where z is the vertical coordinate, g is gravity acceleration, T_a ambient temperature and T_m represents mean gas temperature. Note that Thomas [30] proposed an equation similar to Eq. (2).

The streamlines are determined by the velocity components $U(x)$ and $u(z)$ (Fig. 1) which are very different from one point of the fuel burning particles area to another. Two flows are splitted by the streamline denoted by EB (Fig. 1): the first one which leaves the area through the top (line AB) and the second one which leaves the area through the fire front side (line BC). In order to evaluate the amount of pyrolysis gases of the lower area, only the angle of the tangent in point B is needed. Its expression is then the following:

$$\tan\gamma_{c0} = \frac{U(L)}{u(h)} \tag{3}$$

Considering that the flame time residence τ is inversely proportional to the surface area to volume ratio s ($\tau=\tau_0/s$; τ_0 =75591 [15]) and integrating this differential equation between x=0 –with $U(0) = U$, value of the wind velocity entering the flame base area– and $x = L = R\,\tau$ –when the internal stream leaves the flame base area, x is equal to the flame depth L, see Fig. 1)– yields:

$$U(L) = Ue^{-KR} \tag{4}$$

Table 1
Nomenclature of the model variables and fuel bed characteristics.

Latin symbols		
a_0	Convection coefficient (m^{-1})	=0.4
B	Stefan-Boltzmann constant (W m^{-2} K^{-4})	=5.6×10^{-8}
c	Char rate	=0.15
c_w	Wolff et al. model parameter	
C_p	Specific heat of fuel (J kg^{-1} K^{-1})	
C_{pa}	Specific heat of air (J kg^{-1} K^{-1})	=1150
d	Fuel particle diameter (m)	
D	Distance between two fuel particles (m)	
dx	Elementary fuel cell thickness (m)	
g	Gravity acceleration (m s^{-2})	=9.81
h	Fuel bed depth (m)	
H	Flame height (m)	
k	Catchpole et al. model parameter	
K	Law for drag forces	
K^*	Intermediate drag coefficient	
K_1	Drag coefficient	=7
L	flame depth (m)	
m	Fuel moisture content	
q	Ignition energy (kW m^{-1})	
R	Rate of fire spread (m s^{-1})	
R_b	Contribution of radiation of burning fuel bed to the ROS (m s^{-1})	
R_c	Contribution of convection to the ROS (m s^{-1})	
s	Surface area to volume ratio of fine fuel (m^{-1})	
S	Leaf area by square meter (m^2 m^{-2})	
s_{tb}	Air-pyrolysis gases mass ratio in the flame base	=9
s_{tc}	Air-pyrolysis gases mass ratio in the flame body	=17
T	Mean flame temperature (K)	
T_a	Ambient temperature (K)	=300
T_i	Ignition temperature (K)	=600
T_m	Mean gas temperature (K)	
T_v	Mean fuel temperature (K)	
U	Normal wind velocity (m s^{-1})	
$U(x)$	Air stream velocity within the burning fuel bed (m s^{-1})	
u_c	Upward gas velocity at mid-height vegetal stratum (m s^{-1})	
W	Fire front width (m)	
Greek symbols		
β	Packing ratio	
γ_c	Angle defined in Fig. 1 (°)	
ε_b	Flame base emissivity	
χ_0	Radiant factor	=0.3
ΔH	Heat of combustion of the pyrolysis gases (J kg^{-1})	=1.74×10^7
Δh	Heat of latent evaporation (J kg^{-1})	=2.3×10^6
ρ_v	fuel particle density (kg m^{-3})	
σ	Fuel load (kg m^{-2})	
φ_b, φ_c	Radiative flux, convective flux per unit length (W m^{-2})	
ω	Fuel particle tilt angle (°)	
τ_0	Flame residence time parameter	=75591
τ	Flame residence time (s)	

with

$$K = \frac{K^*\tau_0}{s} \tag{5}$$

where R is the rate of spread (ROS) and K is a drag coefficient which depends on the surface area to volume ratio s.

As the temperature of the fresh airstream entering into the flame is equal to ambient temperature and assuming that the pyrolysis gases temperature is close to the flame temperature, the expression of T_m which depends on the air-pyrolysis gases mass ratio s_{tb} in the flame base is obtained thanks to a weighted average formula:

$$T_m = \frac{s_{tb}T_a + T}{s_{tb}+1} \tag{6}$$

where T is the flame temperature. The value of the coefficient s_{tb} –called stoichiometric coefficient in Balbi et al. [31,32]) is equal to 9. The expression of the mean flame temperature was set in [27,31]:

$$T = T_a + \frac{\Delta H(1-\chi_0)}{(s_{tc}+1)C_{pa}} \tag{7}$$

where ΔH is the heat of combustion of the pyrolysis gases (equal to 1.74×10^7 J kg^{-1} [33]), C_{pa} is the specific heat of air (usually equal to 1150 J kg^{-1} K^{-1}), χ_0 is a radiant factor (equal to 0.3 [34]) and s_{tc} is the air-pyrolysis gases mass ratio in the flame. In presence of ambient wind, the amount of air dragged into the flame may be different from the stoichiometric requirement, due to different mixing efficiency –increase of shear stress, flame stretching–. Indeed, Quintiere and Grove [35] or Ma and Quintiere [36] suggested that the amount of air dragged into the flame may be much higher than the stoichiometric requirement. The value of the coefficient s_{tc} is a universal coefficient which is fitted on one set of experiments (s_{tc} =17).

2.3. Convective preheating intensity

The contact flame (BIB'C'C on Fig. 1) which gets out through the front face of the base is supplied with air/pyrolysis gases mixture coming from the area denoted by (BCDE) on Fig. 1. This surface area is difficult to assess because of its complex shape. As the proposed model has to be simple, this area is replaced by the surface area of the triangle (BCF) where the point F is defined thanks to the angle γ_c (Fig. 1) where

$$\tan\gamma_c = \sqrt{2}\tan\gamma_{c0} \tag{8}$$

Indeed, in order to have the two areas close enough to one another (triangle FBC and area DEBC), the angle γ_c must be greater than γ_{c0} and fitting this angle leads to the value of the linear coefficient given in Eq. (8). Note that the angle γ_c does not represent the flame tilt angle. This error is minimized because the tilt angle of the streamline EB is lower than γ_c.

Thus, substituting Eqs. (3) and (4) in Eq. (8) yields:

$$\tan\gamma_c = \sqrt{2}\frac{Ue^{-KR}}{u_c} \tag{9}$$

where the expression of the upward gas velocity u_c depends on the fuel depth (h):

$$u_c = h^{\frac{1}{2}}\left(\frac{g}{(s_{tb}+1)}\frac{\Delta H(1-\chi_0)}{(s_{tc}+1)C_{pa}T_a}\right)^{\frac{1}{2}} \tag{10}$$

The convective heat flux received by the fuel is equal to the product of the heat of combustion of the pyrolysis gases, the pyrolysis gases flux and the absorption percentage. So, the expression of the convective heat flux is

$$\phi_c = \Delta H\left[\frac{\sigma}{\tau}(1-c)\frac{1}{2}h\tan\gamma_c\right]\left(\frac{h}{h+\frac{H}{2}}\right)a \tag{11}$$

where σ is the fuel load, H the flame height and c is the char rate. The flame height modelling is given by Balbi et al. [31].

The coefficient a takes into account lateral heat losses. If the wind tunnel has lateral walls, there is no lateral heat losses and the coefficient a is equal to 1. Without lateral walls, the amount of lateral energy losses depends on the fire front width (W) in the following way:

$$a = \min(a_0 W; 1) \tag{12}$$

where a_0 is a universal coefficient (a_0 =0.4).

2.4. Flame base radiation

If flame body radiation is negligible due to the fuel bed arrangement –vertically-oriented particles–, the radiation from the flame base remains significant. Its expression is obtained by considering the burnt/unburnt interface (BC on Fig. 1) as a radiant panel. The surface panel is equal to the surface of the projection of the fuel particles and its emissivity is then the projected surface/interface surface ratio. When the fuel bed is composed of vertically-oriented particles, this ratio can be calculated:

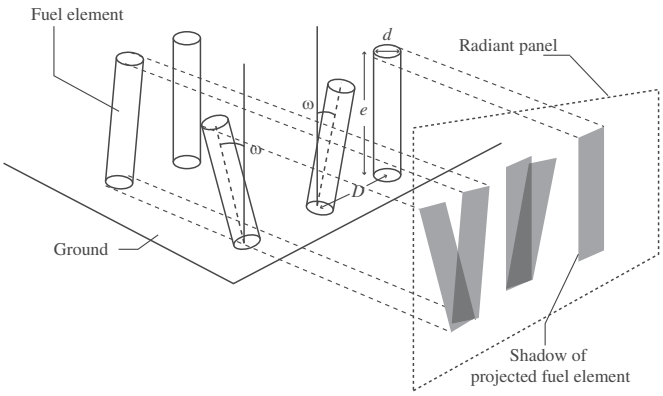

Fig. 2. Main characteristics of the fuel bed arrangement.

$$\varepsilon_b = \min\left[\left(\frac{d}{D} + h\frac{\sin\omega}{D}\right),1\right] \tag{13}$$

where d, D and ω are respectively the particle diameter, the distance between two particles and the particle tilt angle (Fig. 2). Note that the particle tilt angle depends on the fuel particle and the experiments apparati; in most cases, it is practically equal to zero (e.g. [23]) or very small and then the fuel particles are vertically oriented. In some experiments (e.g. [5]) as the particle diameter is smaller than the diameter of the hole in which they are put in, a tilt angle due to the apparatus should not be close to zero and the fuel bed arrangement is practically vertical.

The heat flux provided to the fuel is given by the usual Stefan-Boltzmann formulation for a grey radiant panel:

$$\phi_b = \varepsilon_b B T^4 h \tag{14}$$

where B is the Stefan-Boltzmann constant.

2.5. Preheating thermal balance

Due to the fuel bed arrangement and geometry, flame radiation poorly impinges on the vegetal stratum. So, the thermal balance in a preheated fuel cell is the following:

$$\sigma\, dx\, C_p\frac{dT_v}{dt} = \varphi_b dx + \varphi_c dx - \Delta h\frac{d\sigma_{H20}}{dt}dx \tag{15}$$

where dx is the fuel cell thickness, C_p the specific heat of fuel, T_v the fuel temperature, Δh the heat of latent evaporation, φ_b the radiative flux per length unit and φ_c the convective flux per length unit.

Integrating Eq. (15) over the preheated area and denoting dx/dt by R yields:

$$\sigma[C_p(T_i - T_a) + m\Delta h]R = \int\varphi_b dx + \int\varphi_c dx = \phi_b + \phi_c \tag{16}$$

where m is fuel moisture content and T_i is ignition temperature. Finally, rewriting Eq. (16) yields:

$$R = R_b + R_c \tag{17}$$

with

$$R_b = \frac{1}{\sigma[C_p(T_i - T_a) + m\Delta h]}\phi_b = \frac{\varepsilon_b B T^4}{\beta\rho_v q} \tag{18}$$

where q is ignition energy:

$$q = C_p(T_i - T_a) + m\Delta h \tag{19}$$

and

Table 2
Main wind and fuel bed characteristics of the different sources confronted to the proposed model.

Source	Fuel bed depth (cm)	Surface area to volume ratio (m^{-1})	FMC	Fuel load (kg m^{-2})	Particle diameter or witdh (cm)	Fuel spacing (cm)	Wind (m s^{-1})	Fuel density (kg m^{-3})
Wolff et al. 1991 [5]	4.6	3120	0.08	0.11 to 0.88	0.13	1 to 2	0.4 to 4.6	721
Steward and Tennankore 1979 [37]	6.7 14	329 to 1630	0.06	0.36 to 19	0.25 to 1.91	2.54 3.82	0.242 to 3.48	700
Catchpole et al. 1998 [6]	7.6 15.2	630	0.055 to 0.089	0.61.21	0.6	4.28 4.38	0.45 to 2.68	442
Fons 1946 [12]	14	618 to 1094	0.05 to 0.13	0.51 to 2	0.37 to 0.66	2.54 to 4.45	1.79 to 3.58	418
Finney et al. 2013 [23]	2.5 to 35.6	1590 to 3818	0.1	0.079 to 2.68	0.1 to 1.3	0.64 to 15.7	0.11 to 2.24	600

$$R_c = \frac{1}{\sigma[C_p(T_i - T_a) + m\Delta h]}\phi_c = \frac{\Delta H}{2\tau_0 q}(1-c)sh\frac{h}{h+\frac{H}{2}}a\tan\gamma_c \quad (20)$$

2.6. Model parameters

It is assumed that the drag coefficient K^* is an increasing function of the porosity and a decreasing function of the fuel bed depth:

$$K^* \sim \frac{s\beta}{\sqrt{h}} \quad (21)$$

where β is the packing ratio. Combining Eq. (21) with Eq. (5) yields:

$$K \sim \frac{\beta}{\sqrt{h}} \quad (22)$$

Using Eq. (12), the ratio coefficient is expressed in the following way:

$$K = \frac{K_1}{\min(a_0 W; 1)}\frac{\beta}{\sqrt{h}} \quad (23)$$

where K_1 expresses drag forces.

As previously asserted, the value of the convective parameter a_0, the air-pyrolysis gases mass ratio in the flame s_{tc} and the drag forces coefficient K_1 have been fitted on the experiments carried out by Wolff et al. [5] (s_{tc}=17, a_0 =0.4 and K_1=15). These universal coefficients allow the proposed model to be a predictive model.

Note that due to Eq. (12) if the fire front width is wide enough (W_0 > 2.5 m) or if the experimental apparatus has lateral walls, the convective coefficient a is equal to one and the proposed model only has two universal model parameters (s_{tc} and K_1).

2.7. Model equations

Finally, the rate of spread equation is obtained by rewriting Eq. (17) with Eqs. (12), (13), (18), (19) and (20):

$$R = \frac{\min\left[\left(\frac{d}{D} + h\frac{\sin\omega}{D}\right), 1\right]BT^4}{\beta\rho_v(C_p(T_i - T_a) + m\Delta h)} + \left(\frac{\Delta H}{2\tau_0(C_p(T_i - T_a) + m\Delta h)}(1-c)sh\left(\frac{h}{h+\frac{H}{2}}\right)\min(a_0 W; 1)\frac{e^{-KR}}{u_c}\right)U \quad (24)$$

Note that obviously only the fuel bed characteristics change as well as wind velocity from one experiment to another.

According to Eq. (24), when the normal component of the wind velocity (U) is weak, then the ROS (R) is close to R_b and the exponential function is close to 1. So, the trend of the ROS is practically linear. But when wind velocity increases, ROS increases and the exponential strongly decreases. The ROS behaviour becomes nonlinear and smaller than the linear straight line obtained when U is weak.

3. Numerical results

Many fuels, especially live vegetation canopies are not continuous because they contain gaps of a diameter similar to vegetation clumps. As well-defined fuel beds are less subject to random variations, several studies on wood cribs or well-ordered fuel arrays are reported. Predictions of the proposed model are confronted to the results of 172 laboratory experiments of fire spread carried out in five different references [5,6,12,23,37].

This model is also compared to two other simplified models, namely the models set out by Wolff et al. [5] and Catchpole et al. [6].

3.1. Confrontation to discontinuous fuel bed experiments

The experiments considered here are different from each another: both wind velocity and fuel bed characteristics vary –Table 2 briefly details the main fuel parameters and wind velocities. For instance, Wolff et al. [5] carried out a set of 29 fires with the same fuel bed – White pine toothpicks, *pinus* monticola– except the fuel load which was changed. Steward and Tennankore [37] modified the fuel spacing or the particle diameter and consequently the fuel load in a birch dowels fuel bed. In the 49 fires conducted by Fons (*Pinus ponderosa*) [12], a lot of fuel parameters were changed –Surface area to volume ratio, fuel moisture content, fuel load etc. Finney et al. [23] used a CO_2 laser system in order to cut cardboard fuel elements in an accurate way. This accuracy allows the authors to easily change some fuel parameters –surface-area-to-volume ratio, fuel load, particle diameter, fuel spacing etc. Catchpole et al. [6] have conducted 357 experimental fires over a range of particle sizes, fuel bed depths, packing ratios, moisture contents, and wind velocities. As the primary purpose of this article is to give a convection modelling and to study the trend of the ROS, a group of fires is selected from this substantial number of experiments. Four different fuels were used, of which only the *Pinus ponderosa* (heartwood sticks) experiments are simulated because of their vertically-oriented arrangement.

Error statistics on ROS observations versus predictions were calculated for the model performance study. These include the normalized mean square error (NMSE), an estimate of the overall deviations between predicted and measured values and the Pearson correlation coefficient which is a measure of the linear correlation between predicted and observed ROS. Finally, the fractional bias (FB) is used to estimate the proposed model's under-predictions or over-predictions.

The first results are presented in Fig. 3. The plain line in the scatter diagram represents the line of perfect agreement.

The scatter diagram shown in Fig. 3 indicates that predicted ROS matches measured ROS (NMSE=6.75%) with a bias close to zero (FB=0.05) which means that the proposed model neither overestimates nor underestimates the measured ROS. Note that the NMSE for each

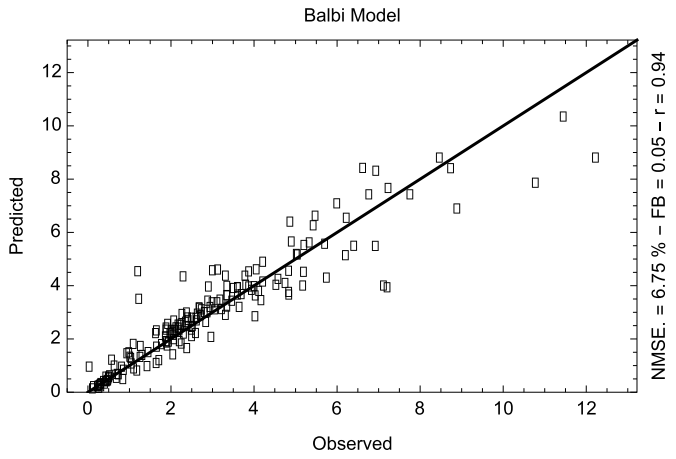

Fig. 3. Predicted ROS given by the proposed model versus observed ROS for the sets of fires spreading in well-ordered and vertically-oriented fuel beds (172 fires).

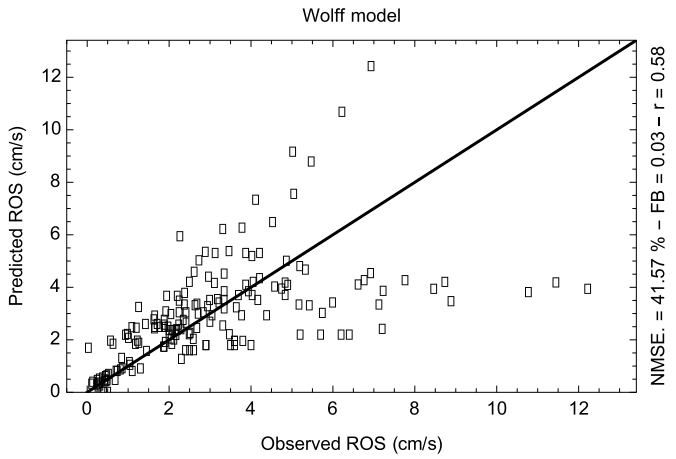

Fig. 4. Predicted ROS given by the Wolff et al. model versus observed ROS for the sets of fires spreading in well-ordered and vertically-oriented fuel beds (172 fires).

set of experiments in Table 3 is low. The value of Pearson's r close to 1 (r=0.94) also indicates a suitable correlation between predictions of the proposed model and experimental ROS. The experiments carried out by Steward and Tennankore [37] are complex to simulate because the ROS trends are different from each another –fast increase, square root trend or very slow increase–. If the proposed model slightly over-estimates the ROS (FB=0.11), the overall performances are satisfactory (NMSE=7.89%, r =0.96).

The mean deviation between the proposed model and the laboratory experiments is weak (NMSE=6.75%). Moreover, a major part of the error only comes from three fires conducted by Finney et al. [23]. Those three fires are not obviously in the general trend of all the other fires of this set of experiments. Removing those fires leads to an NMSE equal to 5.58% for the Finney et al. set of experiments and to 5.13% for all the experiments, which is in the margin of error measurements. Below this threshold, the exact agreement does not make any sense.

3.2. Comparison with other simplified models

The predictions of the proposed model are compared with those from Wolff et al. [5] and Catchpole et al. [6]. In these two simplified models a power law function matches the ROS dependence on wind velocity.

Carrier et al. [38] developed a simple model for the ROS of a fire propagating across an array of fuel particles. Wolff et al. [5] extended this work by taking into account the varying fuel depth. This model is based on the assumption that the dominant heat transfer process is convective heating and is also described by Eq. (25) where c_w is a model parameter, in the present notations.

$$R = c_w \left(\frac{U}{\sigma}\right)^{\frac{1}{2}} (hs)^{\frac{2}{3}} \tag{25}$$

The value that best matches data sets and model performance results are respectively reported in Table 3. The numerical predictions from Eq. (25) are compared with the observed ROS in Fig. 4. Note that thanks to the square root dependence of the wind velocity, the predicted ROS fits the data well when the ROS curve presents a slow increase. The value of the Wolff model parameter which is the best fit for all data sets is equal to 0.07. But the model performances are poor (NMSE=41.57% with a bad correlation coefficient r=0.58).

Catchpole et al. [6] built a predictive model for the ROS based on energy conservation and experimental laboratory fires, which depend on the wind velocity and fuel bed properties. In the present notations, where k is the moisture damping coefficient:

$$R = \frac{(495 + 1934U^{0.91})}{\rho_v \sqrt{\beta}(C_p(\mathrm{T}_i - T_a) + m\Delta h)} e^{-km} \tag{26}$$

The moisture damping coefficient (k) is the only parameter determined from the tuning. Catchpole et al. suggested that it might depend on packing ratio, fuel particle size, or both. If the values of k are known for each fuel type, the model is fully predictive. The value of k which best fits the five experimental data sets is equal to 11. This simplified model is then fully predictive but the results are poor (Table 3) with a large error (46.69%) and a bad correlation (r =0.56).

In comparison with these two simple models, the proposed model provides a better correlation between predicted and observed ROS over a wide range of fuel bed properties (see Figs. 3–5). Not only the precision, but the trend of the ROS is accurately reproduced. Examples

Table 3
Comparison of normalized mean square error (NMSE), fractional bias (FB) and Pearson's correlation coefficient (r) obtained by three simplified ROS models when simulating the experiments carried out by various authors.

Source	nb of fires	Main varying parameters (other than wind)	Proposed model			Wolff et al. model (model param. c_w=0.07)			Catchpole et al. model (model parameter k=11)		
			NMSE (%)	FB	r	NMSE (%)	FB	r	NMSE (%)	FB	r
Wolff et al. 1991 [5]	29	Fuel load	4.15	−0.11	0.96	38.21	0.42	0.97	38.6	0.32	0.95
Steward and Tennankore 1979 [37]	48	Fuel spacing Particle diameter	7.89	0.11	0.96	18.19	0.26	0.91	15.47	0.35	0.94
Catchpole et al. 1998 [6]	20	Fuel depth	2.11	0.05	0.96	81.83	−0.76	0.88	33.46	−0.33	0.79
Fons 1946 [12]	49	Surface-to-volume ratio	1.95	0.05	0.91	4.53	0.09	0.82	19.22	0.13	0.59
Finney et al. 2013 [23]	26	Surface-to-volume ratio	8.74	0.10	0.86	68.7	−0.36	0.78	107.8	−0.78	0.77
Sticks experiments			**6.75**	0.05	0.94	**41.57**	0.03	0.58	**46.69**	0.03	0.56

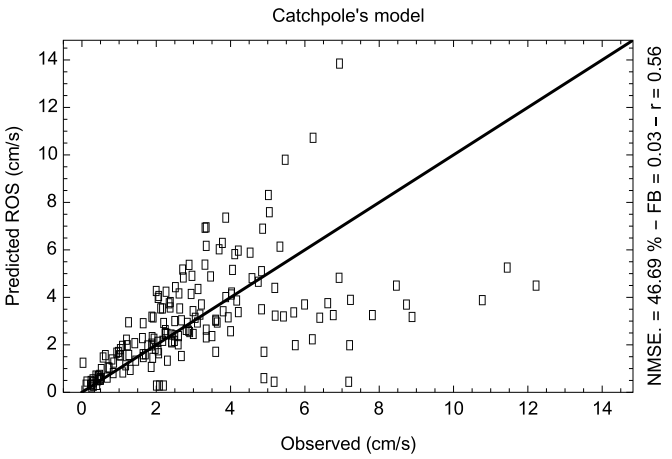

Fig. 5. Predicted ROS given by the Catchpole et al. model versus observed ROS for the sets of fires spreading in well-ordered and vertically-oriented fuel beds (172 fires).

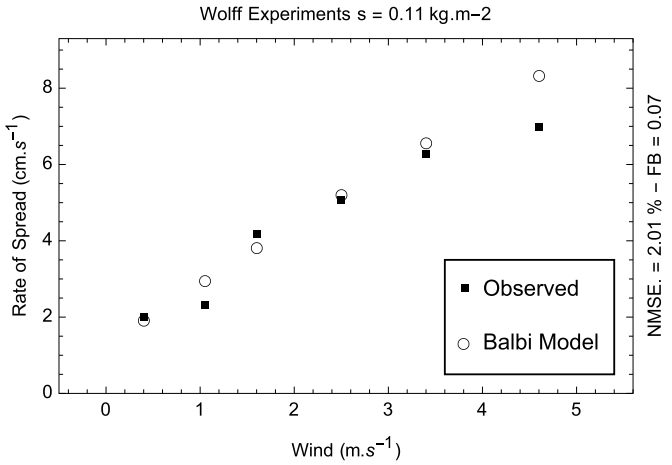

Fig. 6. Predicted ROS given by the proposed model versus observed ROS for a set of experiments carried out by Wolff et al. with a 0.11 kg m^{-2} fuel load.

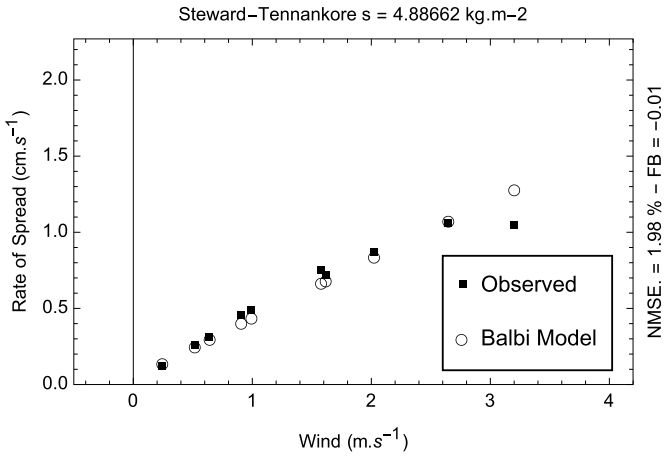

Fig. 7. Predicted ROS given by the proposed model versus observed ROS for a set of experiments carried out by Steward and Tennankore with a 4.88 kg m^{-2} fuel load.

of fires conducted by Wolff et al. [5] and by Steward and Tennakore [37] are presented in Figs. 6 and 7 respectively. In some Steward and Tennakore experiments, the ROS becomes faster as the wind velocity increases and the proposed model correctly expresses this acceleration of the ROS.

The main difference between the three simplified models is the empirical side of the Wolff et al. and Catchpole et al. simplified models

Moreover, the results given by the proposed model are obtained without any change in the values of the three model parameters whatever the experimental data set. The model is fully predictive with a very fast computational time –about 2 s to simulate all the 172 fires using a MacBook Pro with an i7 processor–.

4. Conclusion

This work deals with the development of a simplified propagation model in fuel beds composed of well-ordered, vertically oriented particles at the laboratory scale. Due to the specific fuel bed arrangement, the flame radiation is weakly caught by the vegetal stratum and thus is neglected. The model takes into account two heat transfer mechanisms, namely the horizontal radiation from the base of the flame –fuel burning particles area– and the convection when a part of the flame directly contacts the unburnt fuel.

The expression of these heat transfer mechanisms is partially obtained with usual physical laws and by using some usual empirical laws. The proposed model is constituted by an algebraic relationship of the ROS which depends on the wind velocity, fuel characteristics – moisture content, packing ratio, thickness, width, surface area-to-volume ratio, density etc...– and three universal model parameters – a drag coefficient K_1, a convection coefficient a_0, an air/pyrolysis gases mass ratio s_{tc}–. The important fact is that the value of the three model parameters remains the same whatever the experiments, which means that the model is fully predictive.

The confrontation with 172 laboratory fires found in the literature leads to a small error (less than 7%), a small bias and a proper correlation.

The proposed model is easy to use because of its algebraic structure and then the computational time is close to zero –less than two seconds to simulate all the 172 fires using a MacBook Pro with an i7 processor.

In this work, only fires propagating in fuel beds composed of well ordered and vertically-oriented particles are taken into account. Indeed, these types of fuel bed emphasize the role of convective heating in fire spread. A modelling of this convective heating is given as a flame located into the vegetal stratum which contacts the unburnt fuel. The radiation from the fuel burning particles area is taken into account and due to the fuel bed arrangement, flame radiation is neglected.

Acknowledgments

The present work was supported in part by the French Ministry of Research, the Corsican Region and the National Center for Scientific Research, under Grant CPER 2007–2013. The authors also wish to thank Mr. Pierre Régis Gonsolin for his help in English reviewing.

References

[1] G.M. Byram, Forest fire behaviour, in: K.P. Davis (Ed.)For. Fire Control Use, McGraw-Hill, New York, NY, 1959, pp. 90–123.
[2] W.M. Pitts, Wind effects on fires, Prog. Energy Combust. Sci. 17 (1991) 83–134. http://dx.doi.org/10.1016/0360-1285(91)90017-H.
[3] D. Morvan, Wind Effects, Unsteady Behaviors, and Regimes of Propagation of Surface Fires in Open Field, Combust. Sci. Technol. 186 (2014) 869–888. http://dx.doi.org/10.1080/00102202.2014.885961.

[4] P.H. Thomas, R.W. Pickard, Fire spread in forest and heathland materials, in: FC Great Britain (Ed.), Rep. For. Res., Her Majesty's Stationary Office (HMSO), London, 1961: pp. 105–108.P.H. Thomas, R.W. Pickard, Fire spread in forest and heathland materials, in: FC Great Britain (Ed.), Rep. For. Res., Her Majesty's Stationary Office (HMSO), London, 1961: pp. 105–108.
[5] M.F. Wolff, G.F. Carrier, F.E. Fendell, Wind-aided firespread across arrays of discrete fuel elements. II, Exp., Combust. Sci. Technol. 77 (1991) 261–289. http://dx.doi.org/10.1080/00102209108951731.
[6] W.R. Catchpole, E.A. Catchpole, B.W. Butler, R.C. Rothermel, G.A. Morris, D.J. Latham, Rate of Spread of Free-Burning Fires in Woody Fuels in a Wind Tunnel, Combust. Sci. Technol. 131 (1998) 1–37. http://dx.doi.org/10.1080/00102209808935753.
[7] R.C. Rothermel, H.E. Anderson, Fire spread characteristics determined in the laboratory, USDA Forest Service, Research Paper INT-30, Intermountain Forest and Range Experiment Station, Ogden, Utah, 1966.
[8] R.C. Rothermel, A mathematical model for predicting fire spread in wildland fuels, USDA Forest Service, Research Paper INT-115, Intermountain Forest and Range Experiment Station, Ogden, Utah, 1972. doi:⟨http://www.snap.uaf.edu/web-shared/JenNorthway/AKFireModelingWorkshop/AKFireModelingWkshp/FSPro Analysis Guide References/Rothermel 1972 INT-115.pdf⟩.
[9] J.M.C. Mendes-Lopes, J.M.P. Ventura, J.M.P. Amaral, Flame characteristics, temperature–time curves, and rate of spread in fires propagating in a bed of Pinus pinaster needles, Int. J. Wildl. Fire 12 (2003) 67–84. http://dx.doi.org/10.1071/WF02063.
[10] F.A. Albini, A Model for Fire Spread in Wildland Fuels by-Radiation, Combust. Sci. Technol. 42 (1985) 229–258. http://dx.doi.org/10.1080/00102208508960381.
[11] W.R. Catchpole, E.A. Catchpole, A.G. Tate, B. Butler, R.C. Rothermel, A model for the steady spread of fire through a homogeneous fuel bed, in: Proceedings of the IV Int. Conf. For. Fire Res. 2002, Wildl. Fire Saf. Summit, Luso, Coimbra, Portugal, 2002.
[12] W.L. Fons, Analysis of fire spread in light forest fuels, J. Agric. Res. 72 (1946) 93–121.
[13] F.A. Albini, A physical model for firespread in Brush, in: Proceedings of the Elev. International Symp. Combust., The Combustion Institute: Pittsburgh, PA, Berkeley, CA: pp. 553–560. doi:http://dx.doi.org/10.1016/S0082-0784(67)80180-2, 1966.
[14] M.A. Finney, J.D. Cohen, S.S. McAllister, W.M. Jolly, On the need for a theory of wildland fire spread, Int. J. Wildl. Fire 22 (2012) 25–36. http://dx.doi.org/10.1071/WF11117.
[15] H.E. Anderson, Heat transfer and fire spread, U.S. Department of Agriculture, Forest Service, Research Paper INT-69, 1969.
[16] J.B. Fang, An investigation of the effect of controlled wind on the rate of fire spread, Department of Chemical Engineering, Fredericton, Canada, University of New Brunswick, 1969.
[17] C.E. Van Wagner, Conditions for the start and spread of crown fire, Can. J. For. Res. 7 (1977) 23–34. http://dx.doi.org/10.1139/x77-004.
[18] P.G. Baines, Physical mechanisms for the propagation of surface fires, Math. Comput. Model. 13 (1990) 83–94. http://dx.doi.org/10.1016/0895-7177(90)90102-S.
[19] R.O. Weber, Modelling fire spread through fuel beds, Prog. Energy Combust. Sci. 17 (1991) 67–82. http://dx.doi.org/10.1016/0360-1285(91)90003-6.
[20] W. Tang, C.H. Miller, M.J. Gollner, Local flame attachment and heat fluxes in wind-driven line fires, Proc. Combust. Inst. 36 (2016) 3253–3261. http://dx.doi.org/10.1016/j.proci.2016.06.064.
[21] M. Vogel, F.A. Williams, Flame propagation along matchstick arrays, Combust. Sci. Technol. 1 (1970) 429–436. http://dx.doi.org/10.1080/00102206908952223.
[22] J.M. Prahl, J.S. Tien, Preliminary investigations of forced convection on flame propagation along Paper and Matchstick Arrays, Combust. Sci. Technol. 7 (1973) 271–282. http://dx.doi.org/10.1080/00102207308952367.
[23] M.A. Finney, J. Forthofer, I.C. Grenfell, B.A. Adam, N.K. Akafuah, K. Saito, A study of flame spread in engineered cardboard fuelbeds: Part I: Correlations and observations, in: Proceedings of the Seventh International Symp. Scale Model., Hirosaki, Japan, 2013.
[24] T. Beer, Fire propagation in vertical Stick Arrays - the Effects of Wind, Int. J. Wildl. Fire 5 (1995) 43–49. http://dx.doi.org/10.1071/WF9950043.
[25] K.M. Finney, M.A., Cohen, J.D., Grenfell, I.C., Yedinak, Experiments on Fire Spread in Discontinuous Fuelbeds, in: D.X. Viegas (Ed.), Proc. V Int. Conf. For. Fire Res., Figueira da Foz, Portugal, 2006.
[26] M.A. Finney, J.D. Cohen, J.M. Forthofer, S.S. McAllister, M.J. Gollner, D.J. Gorham, K. Saito, N.K. Akafuah, B.A. Adam, J.D. English, Role of buoyant flame dynamics in wildfire spread, Proc. Natl. Acad. Sci. 112 (2015) 9833–9838. http://dx.doi.org/10.1073/pnas.1504498112.
[27] J.-H. Balbi, J.-L. Rossi, T. Marcelli, P.-A. Santoni, A 3D physical real-time model of surface fires across fuel beds, Combust. Sci. Technol. 179 (2007) 2511–2537 (http://dx.doi.org/10.1080/00102200701484449 http://www.tandfonline.com/doi/pdf/10.1080/00102200701484449).
[28] O. Korobeinichev, A. Tereshchenko, A. Paletsky, A. Shmakov, M. Gonchikzhapov, D. Bezmaternykh, L.Y. Kataeva, D.A. Maslennikov, N. Liu, The velocity and structure flame front at spread of fire across the pine needle bed. Experiment, in: D.X. Viegas (Ed.)Adv. For. Fire Res., Imprensa da Universidade de Coimbra, Coimbra, 2014, pp. 451–458. http://dx.doi.org/10.14195/978-989-26-0884-6_52.
[29] W.R. Anderson, E.A. Catchpole, B.W. Butler, Convective heat transfer in fire spread through fine fuel beds, Int. J. Wildl. Fire 19 (2010) 284–298. http://dx.doi.org/10.1071/WF09021.
[30] P.H. Thomas, The size of flames from natural fires, Symp. Combust. 9 844–859. doi:http://dx.doi.org/10.1016/S0082-0784(63)80091-0, 1963.
[31] J.-H. Balbi, F. Morandini, X. Silvani, J.B. Filippi, F. Rinieri, A physical model for wildland fires, Combust. Flame. 156 (2009) 2217–2230. http://dx.doi.org/10.1016/j.combustflame.2009.07.010.
[32] J.-H. Balbi, J.-L. Rossi, T. Marcelli, F.-J. Chatelon, Physical modeling of surface fire under nonparallel wind and slope conditions, Combust. Sci. Technol. 182 (2010) 922–939 ⟨http://www.tandfonline.com/doi/abs/10.1080/00102200903485178⟩.
[33] R.A. Susott, Characterization of the thermal properties of forest fuels by combustible gas analysis, For. Sci. 28 (1982) 404–420 ⟨http://www.ingentaconnect.com/content/saf/fs/1982/00000028/00000002/art00029⟩.
[34] K.B. Mcgrattan, H.R. Baum, A. Hamins, Thermal radiation from large pool fires, Natl. Inst. Stand. Technol. NISTIR 6546 (2000).
[35] J.G. Quintiere, B.S. Grove, A unified analysis for fire plumes, in: Proceedings of the 27th Symp. Combust., Combustion Insitute, Pittsburgh, PA: pp. 2757–2766. doi:http://dx.doi.org/http://dx.doi.org/10.1016/S0082-0784(98)80132-X, 1998.
[36] T.G. Ma, J.G. Quintiere, Numerical simulation of axi-symmetric fire plumes: accuracy and limitations, Fire Saf. J. 38 (2003) 467–492. http://dx.doi.org/10.1016/S0379-7112(02)00082-6.
[37] F.R. Steward, K.N. Tennankore, Fire spread and individual particle burning rates for uniform fuel matrices, Fire Science Centre, Fredericton, Canada, University of New Brunswick, 1979.
[38] G.F. Carrier, F.E. Fendell, M.F. Wolff, Wind-Aided Firespread across Arrays of Discrete Fuel Elements. I. Theory, Combust. Sci. Technol. 75 (1991) 31–51. http://dx.doi.org/10.1080/00102209108924077.